Experimental Investigation of the Flow Control of Wake Cylinder by a Plate with Different Geometrical Ends

A. B. Khoshnevis
Department of Mechanical Engineering,
University of Hakim Sabzevari, Iran
E-mail: Khosh1966@yahoo.com

A. R. Mamouri*
Engineering Faculty,
Eshragh Institute of higher Education, Bojnourd, Iran
E-mail: amirelmir3000@yahoo.com
*Corresponding author

V. Barzenoni
Department of Mechanical Engineering,
University of Hakim Sabzevari, Iran
E-mail: v.barzanooni@gmail.com

Abstract: An experimental study was carried out on the wake of a cylinder on the back of which a plate is installed parallel to the fluid flow, with different terminal angles, where the Reynolds number is 50000. At the end of the plate, blades with the height of 0.25 equal to the cylinder diameter and with 45, 90 and 135 degrees angle from the horizon, are installed where the cylinder diameter is equal to the plate length. The plate effects on the variation of drag coefficient, medium velocity profiles, reduced velocity, half of the entrance, turbulence intensity and Strouhal number are investigated. The results showed that the drag coefficient for cylinder including the plate, regardless of the end angle, is smaller than the isolated cylinder. The existence of a plate with a terminal angle of 45 degree led to more reduction in drag coefficient of the cylinder.

Biographical notes: A. B. Khoshnevis is an associate professor of Mechanical Engineering at Hakim Sabzevari University, Sabzevar, Iran. He received his PhD from Indian Institute of Technology of Madras Chennai (2000), India, MSc from Indian Institute of Technology of Madras Chennai (1995), and BSc from Ferdowsi University of Mashhad Iran (1990), all in mechanical engineering. His scientific interests includes experimental aerodynamic**. A. R Mamouri** is a PhD student at Faculty of Engineering of Hakim Sabzevari University, Sabzevar, Iran. **V. Barzenoni** is a PhD student at Faculty of Engineering of Hakim Sabzevari University, Sabzevar, Iran.

1   INTRODUCTION

Fluid flow around a circular cylinder is frequently used as a simple model of bluff bodies due to the complexity of the numerical solution of the governing equations, especially in high Reynolds despite its simple geometry, and has been the point of a lot of attention and research. In addition, there has been lots of experimental and numerical research in the area. Transfer of sequence in the hub body, especially cylinders, is important due to making it possible to recognize the different transmission routes into the tangled area, and sheds light on the effect of surface modification on the downstream transmission. Vortices and vortex shedding phenomena play important roles in creating boundary layer and wake. For this reason, knowing the structure and wake of transmission and how they are controlled, is necessary for studying the controlled production structure, the evolution and the deformation of the vortex. With respect to the effect of vortex shedding phenomenon on the drag coefficient, lift trail and turbulence of wake, active and passive techniques for controlling large vortex structures in the flow around circular cylinder has been used. Among these techniques, acoustic stimulation technique [1], heating cylinder [2], swing cylinder at the proper frequency or frequency modulation [3], blowing and suction [4], [5] and electromagnetic control in liquid metal flows [6] can be named. Moreover there have also been several discussions related to separators pages [7] and positive effect on the trail and vortex shedding phenomenon and etc. Changing the type of porous cylinder is also examined [4-8]. A new numerical method such as trust-region and POD [9] were recruited to reduce model rank. Since theoretical methods are still away from practical engineering designs, conducting experiments with wind tunnel is almost the only way to correctly determine the flow parameters like the intensity of turbulence and wake of velocity changes.

In general, to measure the velocity, Pitot tube is utilized, which unfortunately loses its efficiency in flows with high turbulence. That is why, in the present study; one-dimensional hot-wire anemometer is employed to measure the flow parameters. This device is made by Saba Farasanjesh Company and can measure flow turbulence intensity up to 30 KHz. The mechanism of probe transfer is also three dimensional and has a precision of about 0.1 mm.

Practical techniques to measure the coefficient of drag force are divided into several methods. The method utilized in the present study is Wake-Survey. The basis of this method is the difference in the momentum both in the front and in the back of the object.

To measure the velocity, Pitot tube is utilized, which unfortunately loses its efficiency in flows with high turbulence. That is why, in the present study, one-dimensional hot-wire anemometer is employed to measure the flow parameters. The novelty of this paper is that the effects of plate with different geometrical ends on the interaction wake of behind the cylinder with a thin turbulent boundary layer have been investigated experimentally using hot wire anemometry (HWA).

2   LABORATORY EQUIPMENT

In the present study, all of the experiments were carried out in a wind tunnel. The wind tunnel was made of blowing open circuit type with 7 kW power. In order to conduct this experiment, a Plexiglas chamber of 150 cm long, 40 cm wide, and 15 cm high was fabricated (See Fig. 1). The velocity of the wind tunnel can be altered from 0 to 30 m/s by changing the velocity of the installed fan. In the present study, a constant value in each of the experiments is selected for the production capacity. Based on the features of the wind tunnel, the maximum nominal turbulence of the free flow for this device is 0.1%, which results in a high degree of precision. To measure the flow parameters, a constant-temperature hot-wire anemometer was utilized. This anemometer can measure the mean velocity, turbulence, frequency, and exiting vortices from the back of the model. The wind tunnel and the hot-wire anemometer device were both made by Farasanjesh Saba Company. The probe utilized in the present study was one-dimensional and had a sensor with a length of 1.25 mm and diameter of 5μm. The experiments were conducted in summer and the calibration of the devices was carried out at room temperature of T=25°. The room temperature was changing during the day, but the changes were in the range of 2° which is acceptable. In their study, Salari et al., [10] investigated the effects of temperature changes of the free flow (the tunnel temperature) on characteristic curve and calibration of hot-wire sensors.

The results of their study indicated that with an increase in the tunnel temperature, the high voltage of Wheatstone Circuit Bridge in HWA device drops, and the rate of its decrease, depends on the physic of the sensors, velocity flow, and the ratio of the test ultra-heat.

In practice, heat correction coefficients are used to correct this effect. Moreover, the results of investigating the effects of temperature sensor showed that calibration curves achieved for each sensor in different ultra-heat ratios can be matched by applying appropriate correction coefficients. The value for this correction coefficient for HWA at velocity of U=20 m/s is equal to n=0.605, and by applying it in Eq. 1, the real corrected voltage can be solved, and the real flow speed

can be measured using the calibration curve of the sensor [10].

$$\frac{E_r}{E} = \left[\frac{T_w - T_r}{T_w - T_a}\right]^n \tag{1}$$

To move the probe in different locations, a traverse with displacement precision of 0.01 mm and 3 degrees of freedom was utilized [11]. This mechanism moves perpendicular to the free flow and records the required data (See Fig. 2). It is installed on a frame separate from the legs of the wind tunnel so that the probable vibrations of the wind tunnel body does not transfer to the traverse mechanism and data collection takes place with higher quality.
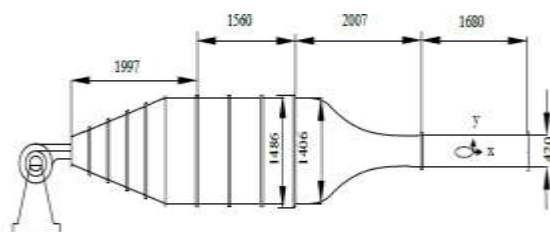
Fig. 1 Schematic of the wind tunnel

The tested blades had 125 mm height and 50 mm length. A solid separator plate places at the end of the cylinder, and the effect of its distal angle on pressure distribution of the cylinder surface, the wake of velocity, and the changes in drag coefficients were investigated. The angle of the distal blades of the plate was 90, 45, and 135° and the length of the plate is 5 cm which is equal to the cylinder diameter. As observed in Fig. 2, data collection was carried out in three longitudinal locations of x/d=0.5, 0.25, and 1 from the end of the sheet, where x is the distance from the end of the plate and d is the cylinder diameter. Reynolds number is 50000 and the input flow speed is 17.5 m/s. To evaluate the correctness of the collected data, the pressure of the cylinder surface was measured without

the plate, and the result was compared with the works that had previously been conducted. The pressure of the cylinder surface was also calculated for different conditions. In so doing, the cylinder surface was divided into 16 equal parts, and by creating holes and connecting them to the barometer, the pressure of different distal parts of the model was measured.
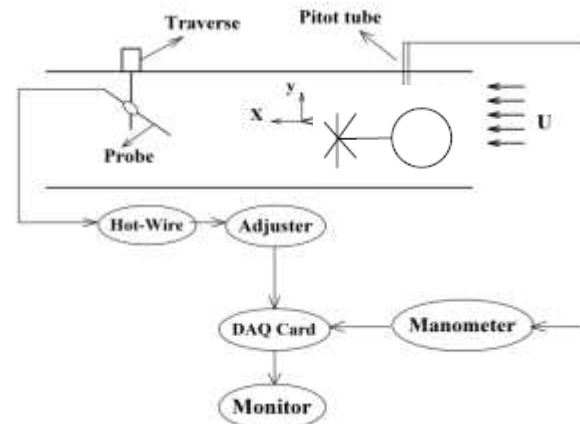
Fig. 2 A schematic of the probe traverse mechanism and how data collection is carried out behind the model
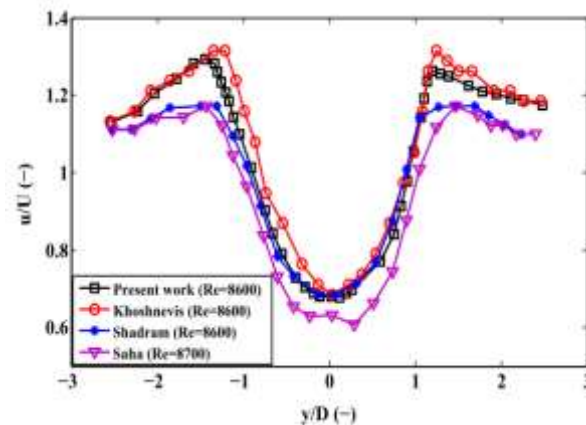
Fig. 3 Profile of average speed for the square cylinder in two different sections

3 VALIDATION

First, a sample data collection was carried out on the performances correctness of the wind tunnel device and hot-wires flow meter, and the results were compared with the studies that had previously been conducted. Since no similar studies had previously conducted on the selected models in this study, a cubic cylinder model was utilized. Fig. 3 presents an average time diagram for speed component in the dominant flow direction of (Ū) for a sample cubic cylinder with a ratio of b/h=1 and in Reynolds number of 8,600 in two

different sections. As it is seen, there is a relatively good match between the present results and the results obtained by Saha et al., [12] and also Shadaram et al., [13] which have approximately the same Reynolds number (It is worth to note that this matter is presented here just as a validation to our results).

4   GOVERNING EQUATIONS

There are several practical techniques to calculate the drag force coefficient. The method used in this research is the Wake-Survey approach and it is based on the momentum difference in the front and back of the object. Measuring velocity is usually done by means of Pitot tube which is unfortunately not practical in highly turbulent flows. Therefore, in this research a hot wire anemometer has been used to measure flow parameters. The equations used to measure drag force are readily extractable by implementation of momentum and mass conservation laws in a control volume. In 1936, Goldstein [14] published his research results regarding the investigation of turbulence intensity and fluid flow fluctuations effects on drag coefficient calculation.

Chao [15] has had many researches investigating turbulence effects on drag coefficient calculation. Rajagopalan [16] has also surveyed the effects of turbulence and fluid fluctuations and gained interesting results. Antonia [17] has done extensive research to investigate the effects of fluid's turbulence rate on the drag force measurement. Van Dam [18] obtained an equation to calculate the drag force coefficient in which the Reynolds stress and fluid turbulence intensity were present, but the fluid's density variations and viscous terms were neglected. The whole equation is as follows:

$$C_d = \int\left(\frac{p_{s,a}-p_{s,w}}{q_\infty}\right)d\left(\frac{y}{l}\right) + 2\int\frac{\bar{u}}{U_\infty}\left(1-\frac{\bar{u}}{U_\infty}\right)d\left(\frac{y}{l}\right) - 2\int\frac{\overline{u'^2}}{U_\infty^2}d\left(\frac{y}{l}\right), \quad (2)$$

As it is seen, this equation is comprised of three parts:
1. Pressure:
$$\int\left(\frac{p_{s,a}-p_{s,w}}{q_\infty}\right)d\left(\frac{y}{l}\right),$$
2. Momentum:
$$2\int\frac{\bar{u}}{U_\infty}\left(1-\frac{\bar{u}}{U_\infty}\right)d\left(\frac{y}{l}\right),$$
3. Reynolds stress:
$$2\int\frac{\overline{u'^2}}{U_\infty^2}d\left(\frac{y}{l}\right).$$

According to Goldstein research:
$$p_{s,a} = p_{s,w} + \bar{q}',$$

$$\bar{q}' = \frac{1}{2}\rho(\overline{u'^2}+\overline{v'^2}+\overline{w'^2}).$$

If above equation is satisfied in equation (2), the following expression would be obtained:

$$C_d = 2\int\sqrt{\frac{\bar{q}}{q_\infty}}\left(1-\sqrt{\frac{\bar{q}}{q_\infty}}\right)d\left(\frac{y}{l}\right) + \frac{1}{3}\int\frac{(\overline{v'^2}+\overline{w'^2}+\overline{u'^2})}{U_\infty^2}d\left(\frac{y}{l}\right), \quad (3)$$

And assuming $u'=v'=w'$ the following equation is reached:

$$C_d = 2\int\sqrt{\frac{\bar{q}}{q_\infty}}\left(1-\sqrt{\frac{\bar{q}}{q_\infty}}\right)d\left(\frac{y}{l}\right) + \frac{1}{3}\int\frac{\bar{q}'}{q_\infty}d\left(\frac{y}{l}\right), \quad (4)$$

In which:

$$\bar{q}' = \frac{1}{2}\rho(\overline{u'^2}+\overline{v'^2}+\overline{w'^2}).$$

Since the model in experiment is two dimensional in a way that flow is only along the test chamber, thus only u', v' parameters are present in the wake of model (the tested model is extended alongside the test section's width and is totally attached to the lateral surface of the test section on both sides and no flow can pass the lateral section of the model.

The flow passes merely over the model in experiment. The equation 4 is also obtained to calculate the drag coefficient in the two dimensional model. Therefore, these equations can be used to measure the drag force coefficient by means of Wake-Survey approach inside the air tunnel and the results are valid [18].

In this research, equation (4) is used to measure the drag force coefficient. The velocity defect, W_0 and half width $b_{1/2}$ parameters are shown in Fig. 4. The velocity defect and turbulence intensity parameters are calculated using bellow correlations:

$$\%Tu = \frac{\sqrt{\overline{u'^2}}}{U_\infty}\times 100 \quad (5)$$

$$W_0 = \frac{U_\infty - U_{min}}{U_\infty} \quad (6)$$

These experiments are done in three stages which are: First stage; installation of the cylinder with a terminal angle of 45°. In all cases the Reynolds number equals 50000 (measured based on the cylinder's diameter) and turbulence intensity is measured to be 0.1. Then in the second stage a plate with the terminal angle of 90° and lastly a plate with the terminal angle of 135° were installed.
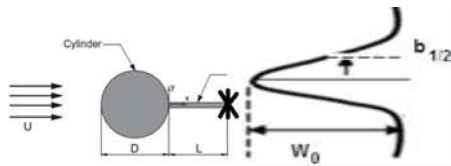
Fig. 4 The velocity defect, W_0 and half width $b_{1/2}$ parameters

5   RESULTS AND DISCUSSIONS

5.1. Velocity wake

Considering the non-dimensional velocity profiles of a single cylinder and a cylinder with plate having different terminal angles, the flow distribution turns more even as the distance from the model increases. In the first station (x/d=0.25), pressure difference is created by potential flow due to the dominance of pressure. In this case, velocity variations from the wake to the potential flow in the top and bottom of model are more intense. In other words, the velocity in the top and bottom of the model faces a severe gradient and U/U_{ref} varies from about 0.3 to 1.3 (U_{ref} is the velocity of free flow or the reference velocity). It is predicted that by gradually increasing the distance from the model, this gradient fades away. A gradual increase of the height in the back of the model, the velocity profile faces a decreasing, increasing and decreasing trend. Figures 5, 6 and 7 show the velocity wake profile of the model in different cases. As it is seen in figure 5, in close distances and when the terminal plane exists, the wake of velocity is higher compared to the isolate case and by increasing the distance from the wake of cylinder, the wake of velocity for the isolate case increases. Terminal angles of 45°, 90° and 135° have the most effect in decreasing the wake of velocity, respectively. At X/D=0.25, the wake of velocity is highest in terminal angles of 45°, 135° and 90°, respectively. However the width of the wake proves the opposite. In the case of X/D=0.5, the velocity values in all cases are almost the same but the wake of width increases in the order of no plate, plate with the angle of 135°, plate with the angle of 45° and plate with the angle of 90°. This can be explained in this way that the terminal angle of 90 creates a barrier in the flow path with larger effective height which causes the wake to get wider. In the case of X/D=1, as it is obvious from the figure, velocity values increase in the order of plate with the angle of 45°, plane with the angle of 90°, plate with the angle of 135° and no plate at all. By increasing the distance of the vector data from the model's extremity in figure 6, it is revealed that the wake of velocity values are approximately fixed for all geometries. More increase in the distance causes the wake of velocity to get higher for 45, 90 and 135

angles, respectively which are in anyway lower than the pressure value of the model's wake in the isolate case.

5.2. Investigation of the wake Turbulence Intensity

Keeping in mind the principle that each moving particle of the fluid always tends to maintain its momentum, when due to a small turbulence or fluctuation, a particle inside the boundary layer jumps from the layer with a low momentum to a layer with high momentum or vice versa without the required potential and merely due to the effect of unstable particles of the fluid, in order for the particle's momentum to be maintained and to some extent get back to the initial value, the particle in its new position, does a small scale movement in the opposite direction of the layer's momentum. All these movements on the whole besides the flow's tendency to keep the continuity law, cause the creation of eddies. The existence of eddy can cause a uniform distribution of momentum, thermal energy, pressure and temperature inside the field. In a flow without any gradient in the average velocity field, a fluctuation in the velocity component does not necessarily turn into an eddy and the mentioned turbulence dissipate shortly under the viscous effects [19].

Figures 8 to 10 show the turbulence intensity at the wake of model for different cases and in different positions in the back of the model. At X/D=0.25 for a cylinder without a plane, turbulence intensity is fluctuating and the amount of fluctuations and turbulence intensity decreases as the distance from the end of the model increases. Generally, in diagrams of turbulence intensity, two peaks of maximum turbulence are evident in the top and the bottom. At X/D=1, the width of the turbulence intensity diagrams are smaller compared to other cases. Altogether, the addition of a plate with different terminal angles leads to a decrease of turbulence intensity compared to a case in which no plane is present.
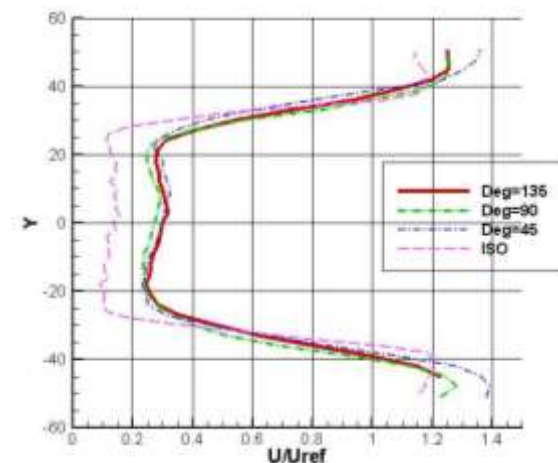
Fig. 5 The wake of velocity profile for the isolate case and three different Terminal Angles x/d=0.25
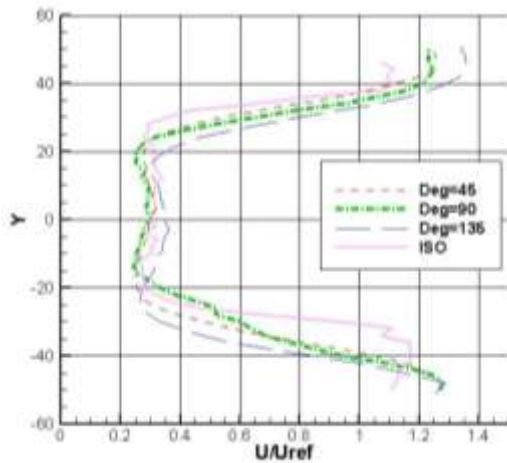
Fig. 6 The wake of velocity profile for the isolate case and three different Terminal Angles x/d=0.5
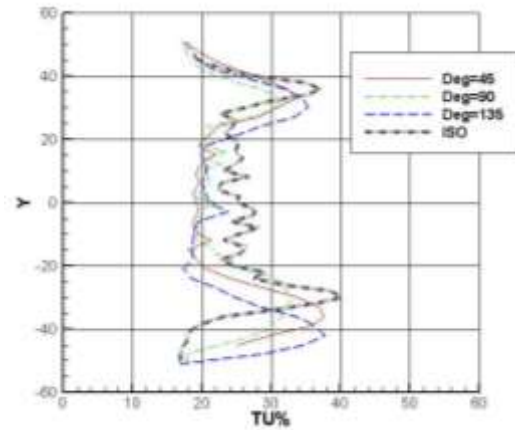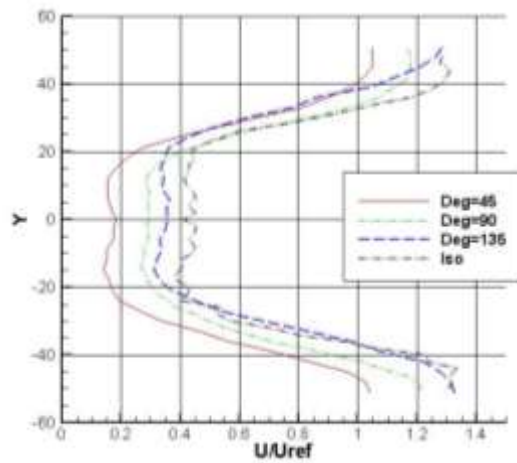
Fig. 7 The wake of velocity profile for the isolate case and three different Terminal Angles x/d=1
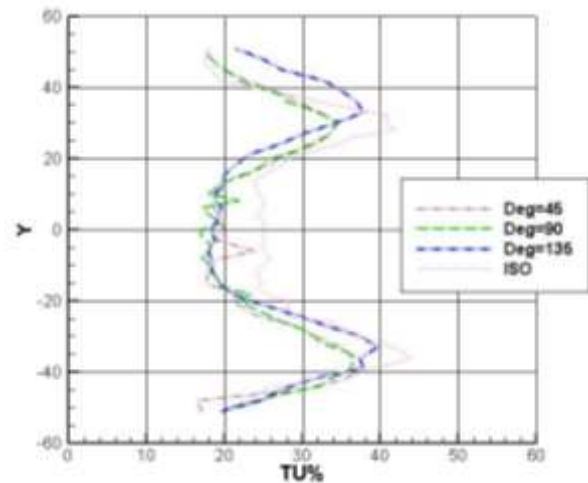
Fig. 8 The wake of turbulence intensity profile for the isolate case and three different Terminal Angles x/d=0.25

Fig. 9 The wake of turbulence intensity profile for the isolate case and three different Terminal Angles x/d=0. 5
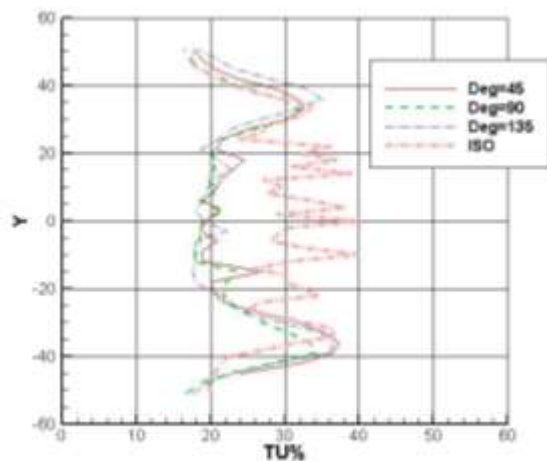
Fig. 10 The wake of turbulence intensity profile for the isolate case and three different Terminal Angles x/d=1

5.3. Velocity defect in the wake

Fig. 11 shows the variations of velocity defect in the wake and Fig. 12 depicts the variations of the half width for a plate with different terminal angles. For various terminal geometries, the velocity defect in the wake first decreases and then increases for a plate with a terminal angle of 45, but for plates with terminal angles of 90 and 135, there is only a decreasing trend. The minimum values of W0 and half width goes to the plate with terminal angel of 135 and the maximum values of W0 and half width relates to the plate with terminal angle of 45 at X/D=1. In distances close to the model, the W0 value increases and the value of the half width also decreases with the increase of the terminal angle. This trend is totally reversed at X/D=1.
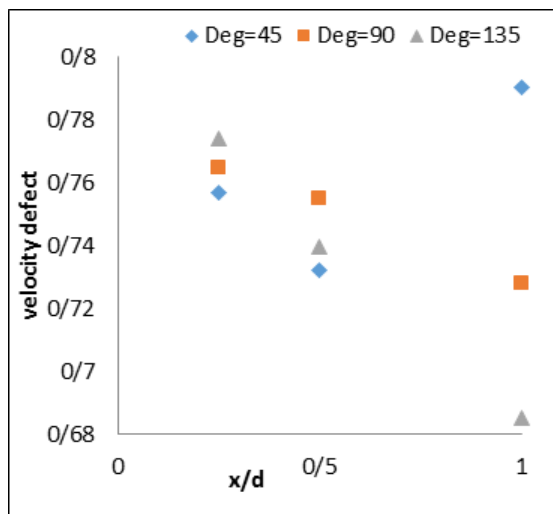
Fig. 11   The variations of velocity defect in the wake for a plate with different terminal angles
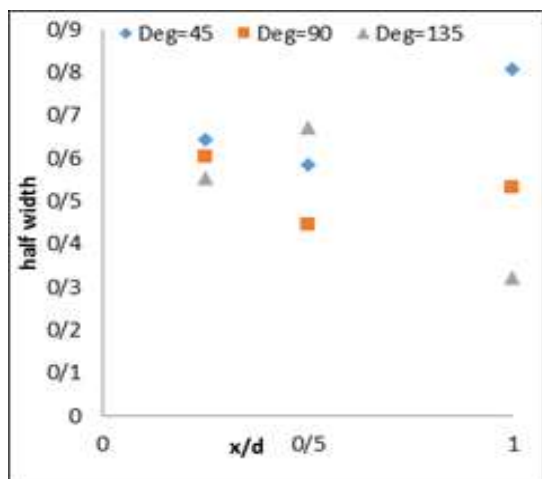
Fig. 12   The variations half width for a plate with different terminal angles

5.4. Strouhal Number

Due to the high frequency response of the hot wire to the speedometer, tachometer is more appropriate than other speedometers. The main benefit of this tachometer is to process the obtained raw from the analysis of the spectral wake of flow charts. Since the hot wire speed saves data anywhere in thousands data stores, getting information from all points of a point is not possible. Somewhat, the spectral analysis of the velocity components in the x, y, and in the selection of the wake reveals dynamic wake. Strouhal number is the dimensionless numbers which constituted Karman Vortex oscillation frequency. Hence, Strouhal number is defined as follows [2]:

$$St = f \times \frac{c}{U_{ref}} \tag{7}$$

Where, f is the frequency of vortex behind the model, and c is the cylinder diameter and Uref is the flow rate of the fluid. Frequency of the vortices formed by the model can be obtained in a wind tunnel by hot-wire flow meter sensor.

5.4.1. Measuring Vortex Frequency Using Hot-Wire Sensor

Hot-wire sensor receives the fluctuations in wind tunnel flow as the time fluctuations or in the time domain and takes it to the frequency domain using Fast Fourier Transform and shows the result as the fluctuation range in terms of oscillation frequency. The vector data frequency in the wind tunnel was set at 5 KHz (See Fig. 13).
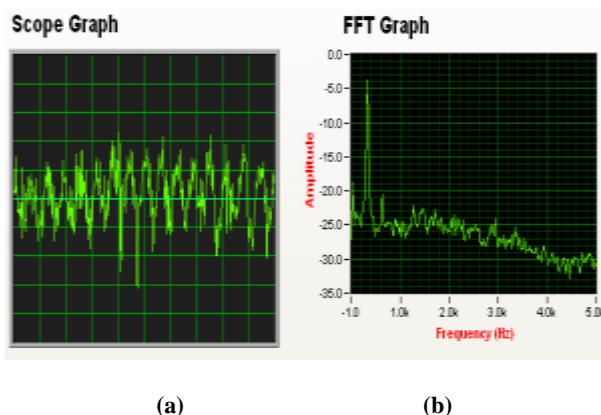
(a)   **(b)**
Fig. 13 (a): fluctuations flow in the time domain; (b): fluctuations flow in the frequency domain

In the frequency domain, the range of all flow fluctuations (with different frequencies) that are measured by the sensor can be observed.
According to figure 14, by examining Strouhal number (Defined by the diameter of the cylinder), it can be seen that the highest value of the mentioned parameter occurs in a cylinder with a 45°-distal-angle plate and at location of X/D=0.05. And, its lowest value is related to a plate of 135° at location D/X=0.25. In all states, the amount of the Strouhal number first rises and then falls with an increase in the distance with the model. Among all fluctuations, Karman vortices have the highest range. Therefore, the frequency related to the highest range is in fact related to Karman vortex. Based on this point, it can be stated that the cylinder with a 45°-distal-angle plate creates vortices with bigger frequencies behind the cylinder.
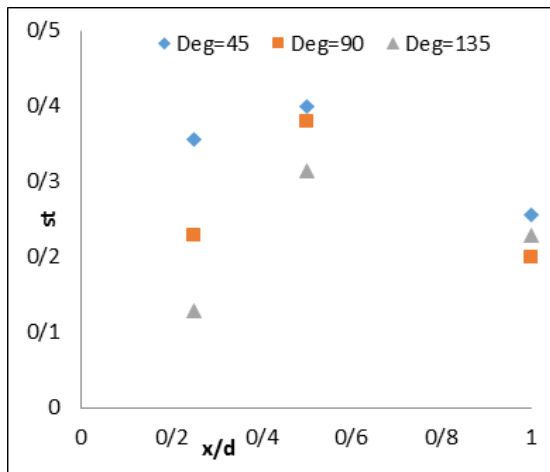
Fig. 14   The variations of the Strouhal number for a plate with different terminal angles

5.5 Pressure Coefficient

In order to confirm the measurements done in the experiment, the pressure profile was calculated on the cylinder without a plane and a good match obtained [20].
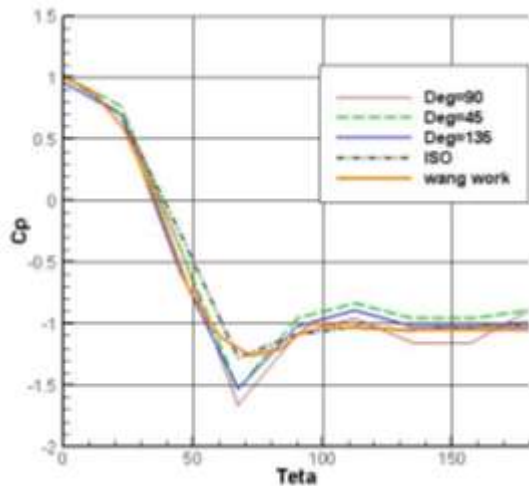
Fig. 15   The variations of the Pressure Coefficient for a plate with different terminal angles

In Fig. 15, it is obvious that the variation of the terminal geometry does not have a major effect on the pressure coefficient in planes with angles less than 60°. However, by increasing the angle, the pressure coefficient would be less in terminal angle of 90 compared to terminal angles of 135 and 45. The terminal angle of 45 causes a pressure coefficient increase on the cylinder surface compared to the isolate case of the model. Terminal angle of 135 does not affect the pressure coefficient that much compared to the cylinder without any plane. Terminal angle 90 would cause a pressure coefficient reduction compared to the isolate cylinder.

5.6. Drag Coefficient

The drag coefficient values for an isolate cylinder and a cylinder with different terminal angles are listed in table 1. The drag coefficient of an isolate cylinder in Reynolds number of 50000 is approximately 0.45 in the reference [21] which has a good match with the results of the present work. By adding a plane to the end of the cylinder, the results showed that the drag coefficient is the highest in the case of a terminal angle of 90 which could be explained in this way that due to the creation of a wider wake area, a greater pressure drop is seen in the back of the model and the momentum component of the drag coefficient increases. Surely, the turbulence component has also been increased compared to other cases which have a minor effect on the final drag coefficient increase.

The important point is that in all cases the drag coefficient is less than that of the cylinder without a plane. The cause of this could be the prevention from the interaction and mixture of the released vortexes in the top and bottom of the model. Although the terminal angles increase the turbulence intensity in the back of the model, but the effect of this turbulences on the drag coefficient increment is less than that of the interaction of the released vortexes in the back of the model. The minimum drag coefficient value is obtained in the case of the terminal angle of 45. The reason for that is somehow the prevention of vortex movements and to a minor effect, the increase in the wake width.

Table 1 The Drag Coefficient for a plate with different terminal angles

Deg=45	Deg=90	Deg=135	isolated	
0.26	0.41	0.281	0.45	CD total
0.17	0.29	0.201	0.31	Momentum term
0.09	0.11	0.08	0.14	Intensity term

6   CONCLUSION

In this study, the wake of a cylinder with a terminal plate consisting of three blades with different mounting angles at the end of the plate and with the Reynolds number, Re = 50000, were examined in the wind tunnel. For measuring the flow parameters, a one-dimensional hot-wire anemometer was used. Based on the points mentioned, the following results were obtained from the conducted experiments:

1) The terminal angle of 90 degree created a barrier with effective height in the direction of flow and thereby led to openness and vastness of the wake.

2) The addition of the plate with different terminal angles reduced the amount of turbulence intensity compared to the state in which no plate was used.

3) For different terminal geometries, the minimum velocity in a wake (W0) for the plate with a 45-degree end angle primarily decreases and then increases, but for 90 and 135 degree angles, the minimum velocity merely had a downward trend.

4) The maximum value of the Strouhal number was in the cylinder with a plate with the terminal angle of 45 degrees and X / D = 0.5 end position, and the minimum value of the parameter occurs in the plate with the terminal angle of 135° and at X / D = 0.25 position. In all cases, the Strouhal number by increasing distance from the model first starts to increase and then decreases.

5) The change in the final geometry of the model has no significant effect on the pressure coefficient at the angles less than 60 degrees. But, by increasing the angle, the coefficient of pressure for the final angle of 90° is less than 135° and 45°.

6) Regardless of the terminal angle, the drag coefficient for cylinder with the plate is smaller than the isolated cylinder. The existence of a plate with a terminal angle of 45-degree angle further reduced the drag coefficient.

7   NOMENCLATURE

Cp	**Pressure coefficient**	
C_D	Drag coefficient	
f	Frequency of vortex shedding	(1/s)
$P_{s,e}$	Static pressure in upstream of model	(pas)
$P_{s,w}$	Static pressure of model wake region	(pas)
q_∞	Dynamic pressure	(pas)
Re	Reynolds number	
St	Strouhal number	
Tu%	Turbulence intensity	
U	Time-averaged velocity	(m/s)
U_{ref}	Free stream velocity	(m/s)
u', v', w'	Velocity fluctuation in x,y,z directions, respectively	(m/s)
W_0	Velocity defect parameter	(m/s)
X, Y	Cartesian coordinates (X-streamwise distance from the cylinder and Y-vertical distance from the bottom plate)	(mm)
x, y	Cartesian coordinates (relative distance from the center of the cylinder)	(mm)
Greek symbols		
μ	Kinematic viscosity of air	$\left(N \cdot s/m^2\right)$
ρ	Fluid density	$\left(kg/m^3\right)$

REFERENCES

[1] Blevins, R. D., "Acoustic Modes of Heat Exchanger Tube Bundles", 1985, Journal of sound and Vibration, Vol. 109, No. 1, 1986, pp. 19-31.

[2] Hamma, J. C. L., Paranthoen, P., "The control of vortex shedding behind heated circular cylinders at low Reynolds numbers", Journal of Experiments in Fluids, Vol. 10, 1991, pp. 224-229.

[3] Bayazitoglu, Y., Sunryanaratana, P. V. R., "Dynamics of oscillating viscous droplests immersed in viscous media", Journal of Acta Mechanica, Vol. 95, Texas 1992, pp. 167-183.

[4] Framsson, J. H. M., Konieczny, P., and Alfredsson, P. H., "Flow around a porous cylinder subject to continuous suction or blowing", Journal of Fluids and Structures, Vol. 19, 2004, pp. 1031-1048.

[5] Zhijin, Li, Navon, I. M., Hussaini, M.Y., and Le Dimet, F.-X., "Optimal control of cylinder wakes via suction and blowing", Journal of Computers & Fluids, Vol. 32, 2003, pp. 149-171.

[6] Mutschke, G., Shatrov, V., and Gerbeth, G., "Cylinder wake control by magnetic fields in liquid metal flows", Journal of Experimental Thermal and Fluid Science, Vol. 16, 1998, pp. 92-99.

[7] Igbalajobi, A., McClean, J. F., Sumnern, D., and Bergstrom, D. J., "The effect of a wake-mounted splitter plate on the flow around a surface mounted finite-height circular cylinder", Journal of Fluids and Structures, Vol. 37, 2013, pp. 185–200.

[8] Yu, P., Zeng, Y., Lee, T. S., Bai, H. X., and Low, H. T., "Wake structure for flow past and through a porous square cylinder", International Journal of Heat and Fluid Flow, Vol. 31, 2010, pp. 141–153.

[9] Bergmann, M., Cordier, L., "Optimal control of the cylinder wake in the laminar regime by trust-region methods and POD reduced-order models", Journal of Computational Physics, Vol. 227, 2008, pp. 7813–7840.

[10] Salari. M, Ardakani. M. A., and Taghavi Zonnor, R., "Experimental Study for Effect of Free Flow Temperature Changes and Hot Wire Anemometer on sensors calibration and Velocity measurement", Journal of Mechanics and AeroSpace, 1384, Vol. 1, No. 3, pp. 49-59 (in Persian).

[11] Ardakani, M. A., "Hot Wire Anemometer", Vol. 1, Khaje Nasiroddin Tosi University, 1385 (in Persian).

[12] Saha, A. K., Muralidhar, K., and Biswas, G., "Experimental Study of Flow Past a Square Cylinder at High Reynolds Numbers", Experiments in Fluids, Vol. 29, No. 4, 2008, pp. 553-563.

[13] Shadaram A., Azimifrad, M., and Rostami, N., "Study of characteristic flow at the near wake of square cylinder", J. of Mechanical- aerospace Vol. 3, No. 4, 1386 (in persain).

[14] Goldstein, S., "A Note on the Measurement of Total Head and Static Pressure on a Turbulent Stream", Proceedings of the Royal Society of London, Series A, Vol. 155, No. 32, 1936, pp. 570-575.

[15] LU, B., Bragg, M. B., "Experimental Investigation of the Wake-Survey Method for a Bluff Body with Highly Turbulent Wake", AIAA-3060, Year 2002.

[16] LU, B., Bragg, M. B., "Experimental Investigation of Airfoil Drag Measurements with Simulated Leading-Edge Ice Using the Wake-Survey Method", AIAA3919, Year 2000.

[17] LU, B., Bragg, M. B., "Airfoil Drag Measurement with Simulated Leading Edge Ice Using the Wake-Survey Method", AIAA1094, Year 2003.

[18] Van Dam, C. P., "Recent Experience with Different Methods of Drag Prediction", Progress in aerospace. Science, Vol. 35, No. 8, 1999, pp. 751-798.

[19] Sanieinejad, M., "Fundamentals of Turbulent Flows and Turbulence modeling", daneshnegar publisher, 978-964-2927-35-337, Tehran 1388 (in Persian).

[20] Wang, J. S., Qiao, X. Q., "Pressure distribution, Fluctuating Forces and vortex shedding behavior of circular cylinder with rotatable splitter plates", Journal of Fluids and Structures, Vol. 12, 2012, pp. 263-278.

[21] Fox, R., Mcdonald, A., "Introduction to fluid mechanics", 4th Ed.